A Letters Journal Exploring the Frontiers of Physics

April 2009

EPL, **86** (2009) 17003
doi: 10.1209/0295-5075/86/17003

www.epljournal.org

Phase transitions, entanglement and quantum noise interferometry in cold atoms

F. Mintert[1,2,3], A. M. Rey[3,4], I. I. Satija[5,6] and C. W. Clark[5,7]

[1] *Physikalisches Institut, Albert-Ludwigs Universität Freiburg - Hermann-Herder-Str. 3, Freiburg, Germany, EU*
[2] *Department of Physics, Harvard University - 17 Oxford Street, Cambridge, MA, USA*
[3] *Institute for Theoretical Atomic, Molecular and Optical Physics, Harvard University - Cambridge, MA 02138, USA*
[4] *JILA and University of Colorado, Department of Physics, University of Colorado - Boulder, CO 80309, USA*
[5] *National Institute of Standards and Technology - Gaithersburg, MD 20899, USA*
[6] *Department of Physics, George Mason University - Fairfax, VA 22030, USA*
[7] *Joint Quantum Institute, National Institute of Standards and Technology and the University of Maryland Gaithersburg, MD 20899, USA*

received 22 July 2008; accepted in final form 5 March 2009
published online 15 April 2009

PACS 73.43.Nq – Quantum phase transitions
PACS 42.50.Lc – Quantum fluctuations, quantum noise, and quantum jumps
PACS 03.75.Hh – Static properties of condensates; thermodynamical, statistical, and structural properties

Abstract – We show that entanglement monotones reveal the pronounced enhancement of entanglement at a quantum phase transition, when they are sensitive to long-range *high-order* correlations. Such monotones are found to develop a sharp interferometric peak at the critical point, and to exhibit universal scaling. We demonstrate that similar features are shared by noise correlation spectra, and verify that these experimentally accessible quantities encode entanglement information and probe separability. We give a prescription, for mesoscopic scale systems of how to extract the pronounced enhancement of entanglement at a quantum phase transition from limited accessible experimental data.

Entanglement, among the most fascinating features of quantum theory, has emerged as an important resource in quantum information science [1]. As entanglement represents a unique form of correlation that does not occur in classical systems, the investigation of connections between entanglement and quantum phase transitions [2–5] is an emerging field of research which seeks to complement the understanding of critical phenomena in condensed-matter physics and quantum field theory.

Iconic examples of solvable models exhibiting quantum phase transitions, such as the Ising-like spin chain, are paradigms for investigating the suitability of proposed entanglement measures, *e.g.* the concurrence and entanglement entropy [6], to quantify the entangling resources of a system close to its quantum critical point. Among the various entanglement measures the concurrence has gained particular attention in view of its universal scaling close to the phase transition [6–8]. However, regular concurrence has the drawback that even at the critical point where spin-spin correlations extend over a long range (as the correlation length is diverging for an infinite system) only the next- and next-to-nearest neighbor concurrences are non-zero. Moreover, it is not concurrence that peaks at the transition but its first derivative.

The expected enhancement of entanglement at a phase transition has been observed using the entanglement entropy S_ℓ between a block of ℓ consecutive spins and the rest of the chain [9,10]. However, there is as yet no systematic understanding of why some entanglement measures capture this enhancement and others do not. A way to resolve the frequent non-appearance of a peak at the critical point was proposed in refs. [11–13] with the help of generalizations of concurrence and the use of symmetry broken states. The latter approach applies in the thermodynamic limit, however cannot be applied to mesoscopic scale systems where there is no actual broken symmetry (but nevertheless exhibit most of the characteristic signatures of a quantum phase transition) or other type of phase transitions without a local order parameter, such as topological phase transitions. Here we

propose a general explanation for the different abilities of various entanglement measures to describe quantum phase transitions using the actual ground state with an eye towards the understanding of systems where the symmetry broken state is not a suitable description. For simplicity, we concentrate our analysis on a chain of interacting spins. Our conclusions are particularly relevant for cold-atom systems, which are only weakly coupled to their environment and are significantly further away from the thermodynamic limit than their condensed-matter counterparts. With the help of a sequence of entanglement measures, we develop a systematic approach that illustrates how correlations are established over different ranges, and the different behavior of long-range *vs.* short-range correlations as the system approaches the critical point. Our study reveals the importance of *higher-order* correlations to determine the entanglement near a quantum phase transition.

Whereas entanglement measures have become common tools for theoretical investigations, they are significantly less popular in the experimental community since they are typically extremely arduous if not practically impossible to measure. For the verification of theoretical findings and for the investigation of theoretically intractable systems it is therefore necessary to have efficient *experimental* means to probe entanglement properties. Among the various physical systems exhibiting quantum phase transitions, cold atoms loaded in optical lattices [14] offer considerable advantages over more traditional examples, since their Hamiltonians can be engineered to high precision, and noise and randomness can be controlled. In these systems, many-body correlations are extractable from absorption images of the atomic cloud after its release from the trap [15,16]. However such images typically do not provide sufficient information to recover a proper entanglement measure. Here we give a prescription of how to extract the pronounced enhancement of entanglement at a phase transition from the limited accessible experimental data.

We consider the ground state of the one-dimensional spin-1/2 anisotropic XY model in a transversal magnetic field characterized by the Hamiltonian

$$\hat{H} = -\frac{J}{2}\sum_{j=1}^{N}(1+\gamma)\sigma_j^x\sigma_{j+1}^x + (1-\gamma)\sigma_j^y\sigma_{j+1}^y + h\sigma_j^z, \quad (1)$$

where J is the nearest-neighbor coupling constant, h is a transverse magnetic field, γ is the anisotropy parameter, $0 \leqslant \gamma \leqslant 1$, σ_j^α are Pauli matrices ($\alpha = x, y, z$) and periodic boundary conditions are assumed throughout. For $0 < \gamma \leqslant 1$, $\hat{H}$ belongs to the Ising universality class, and it exhibits a quantum phase transition from a paramagnetic to a ferromagnetic phase when $\lambda = h/J$ takes its critical value $\lambda_c = 1$ [17]. The XY model is exactly solvable, and any correlation function on the exact ground state can be expressed in terms of Toeplitz-like determinants after a Jordan-Wigner transformation that maps spin operators into fermionic operators [18–20]. The evaluation of *all* four-point correlations is however more cumbersome than the commonly used prescription for computing two-point functions. In ref. [21] we provide specific details on how to calculate these higher-order correlations in hard core boson systems ($\gamma = 0$) with fixed number of particles. This can be straightforwardly generalized to the spin system in consideration via the Holstein-Primakoff transformation [22]. We note however that in the anisotropic spin chain considered in the present work, the effective fermionic Hamiltonian obtained after applying the Jordan-Wigner transformation does not commute with the total number of fermions operator and therefore the number of nonzero higher-order correlation significantly increases.

For bipartite systems, both entanglement entropy and concurrence play an important role, since they are the first monotones that can be evaluated by purely algebraic means for mixed states [23,24]. Entanglement entropy is defined in terms of the degree of mixing of the reduced density matrix ϱ_r of either of the two subsystems: $S(\Psi) = -\mathrm{Tr}\varrho_r \log \varrho_r$, and concurrence's most frequently used definition is given in terms of the second Pauli matrix σ_y, and reads $c(\Psi) = |\langle\Psi^*|\sigma_y \otimes \sigma_y|\Psi\rangle|$, where $\langle\Psi^*|$ is the complex conjugate of $\langle\Psi|$, that is the transpose of $|\Psi\rangle$, with the conjugation/transposition performed in the σ_z eigenbasis. For a system of two spins concurrence and entanglement entropy are equivalent as one is a bijective function of the other. However, for multipartite systems this is no longer the case and there is no unique generalization for either of these measures.

A challenge for investigations of entanglement in many-particle systems is that many-particle entanglement often *cannot* be discovered in terms of few-body correlations alone [7,8]. Therefore, we will not consider entanglement properties of reduced few-body states, but only investigate properties of the ground state of the entire many-body system. In the case of entanglement entropy [9,10] we will divide the spin chain into two blocks of not necessarily consecutive spins and consider the entanglement entropy between those blocks. In the case of concurrence we will use generalizations based on the popular redefinition $c(\Psi) = \sqrt{2(1 - \mathrm{Tr}\varrho_r^2)}$ [25] of concurrence: we will focus on the discrete set of generalized tangles (squared concurrence) [26–28],

$$T_k = 2 - \frac{2}{D_k}\sum_{\nu\in\kappa_k}\mathrm{Tr}\varrho_\nu^2, \quad (2)$$

where the ϱ_ν are reduced density matrices of 1 to k spins, and the summation is performed over all reduced density matrices of up to k spins. Formally, this means that κ_N contains all 1- to k-touples of pairwise distinct elements labeling the individual sites. The constants $D_k = \sum_{i=0}^{k-1}\prod_{j=0}^{i}(N-j)$ are chosen so that fully separable states yield a vanishing value of T_k. The advantage of this choice of entanglement monotone over various alternatives is that it can easily be evaluated in terms of the four-point correlation functions. The average entanglement between

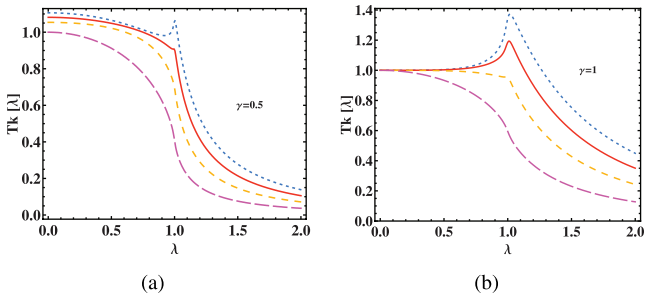

Fig. 1: (Color online) Multipartite variations of the tangle (squared concurrence), as functions of λ for $\gamma = 1$ (right panel) and $\gamma = 0.5$ (left panel), obtained by numerical computation of Toeplitz determinants for a system of size $N = 175$: T_1 long-dashed (pink); T_2 dashed (yellow); T_3 solid (red); and T_4 dotted (blue). T_1 and T_2 do not show a distinct peak near the critical point, $\lambda = 1$.

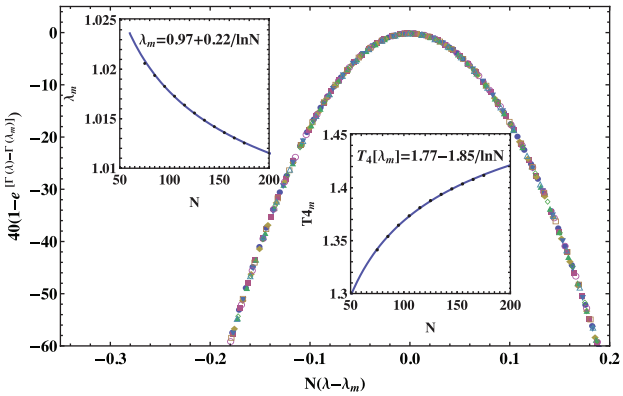

Fig. 2: (Color online) The main plot shows the universality of $\Gamma \equiv (T_4 – T_4^*)^{-1}$ around the phase transition: $\Gamma(\lambda) - \Gamma(\lambda_m)$ is plotted for various system sizes, from $N = 75$ to 175, as function of $N(\lambda - \lambda_m)$, and the same behavior is found for all system sizes that are displayed with different symbols. The insets show the growth (right) and position (left) of the peak with increasing system size.

an individual spin and the rest of the chain is characterized by T_1, T_2 brings in the entanglement between pairs of spins and the residual system, and T_3 and T_4 contain higher-order correlations. This hierarchy extends to the multi-particle concurrence, *i.e* $\{T_1, \ldots T_N\}$, [29] that provides a quantification for the entire entanglement content of a multipartite system. We restrict the present investigation to T_1-T_4, since the evaluation of 5-point quantities becomes impractical for large systems.

A clear difference between the behavior of bipartite and multipartite entanglement can be seen already going from T_1 to T_4. This is shown in fig. 1, where the different multipartite tangles are plotted as functions of λ for $\gamma = 1$, and $\gamma = 0.5$. In neither case do T_1 or T_2 show a distinct peak near the phase transition, but their behavior rather resembles the step-like behavior of the regular concurrence [7]. But starting from T_3 for the case of $\gamma = 1$, and T_4 for $\gamma = 0.5$, there is a clear peak arising around the critical point. As can be seen for $\gamma = 1$ the peak becomes more pronounced with increased order of correlation in T_k. This shows that the long-range correlations that are established around a quantum phase transition are displayed in terms of multipartite entanglement, whereas the bipartite entanglement between blocks of consecutive spins does not display this behavior.

In order to quantify the growth of multipartite entanglement in T_4 at the critical point, we study the scaling with system size of its peak height and position. The right inset of fig. 2 shows the growth of the peak with increasing number of spins. Since T_4 is a bounded quantity, it cannot diverge even in the thermodynamic limit. Nevertheless, it converges to its maximal value following an inverse logarithmic behavior (see solid-line fit). The left inset of fig. 2 shows that, with increasing system size, the position of the peak, λ_m, gets shifted towards the expected value in the thermodynamic limit, $\lambda_m = 1$. However, according to the logarithmic fit that follows the data, λ_m does not asymptote to a value of 1 but rather to 0.97. We do not attribute too much significance to this observation, but rather expect that additional data for larger systems would result in a slightly more accurate extrapolation.

Considering the well-known universal behavior of Ising-like models at a phase transition, it is essential to check whether our presently utilized quantification of entanglement reveals universality. Since by definition T_4 is always finite, a more appropriate quantity to reflect universal scaling is $\Gamma \equiv (T_4 - T_4^*)^{-1}$, since it exhibits a logarithmic divergence at the critical point. Here T_4^* is the maximum value reached by T_4 in the thermodynamic limit at $\lambda_m = 1$, which we calculate to be $\pi/2$. Again T_4^* does not agree exactly with the value of 1.77 we obtain from finite-size scaling; as before we attribute this to the size limitations. Figure 2 shows that $\Gamma(\lambda) - \Gamma(\lambda_m) = f[N^{1/\nu}(\lambda - \lambda_m)]$ exhibits universal behavior with the scaling exponent $\nu = 1$ characteristic for the Ising model [17]. When we plot this quantity as a function of $N(\lambda - \lambda_m)$ for different system sizes, there is an almost perfect coalescence of the various data points onto a single curve. Furthermore, the shape of this universal curve closely resembles the universal curve underlying concurrence [7].

To show that it is the long-range correlations that grow, *vs.* the entanglement between close neighbors, and that our findings above are not artifacts of particular choices of T_i, we consider the case of another well-established entanglement measure, the *entanglement entropy*. In contrast to previous studies [9,10] which considered bipartition of the spin chain into ℓ consecutive spins and the rest of the chain, we study the entanglement entropy, $S_4(L)$, that is extracted by bipartition of the spin chain into four spins that are separated by distance L, (say spin 1, $1+L$, $1+2L$, and $1+3L$) and the rest of the system. This quantity is shown in fig. 3. Note that similarly to T_4, also $S_4(L)$ remains finite in the thermodynamic limit,

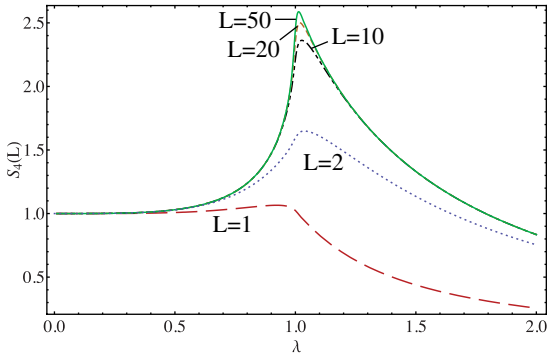

Fig. 3: (Color online) Entanglement entropy, $S_4(L)$, as function of λ for different spacings between the four spins. $S_4(L)$ grows monotonically with increasing separation and reaches its maximum value when $L = N/4$. Here $N = 201$.

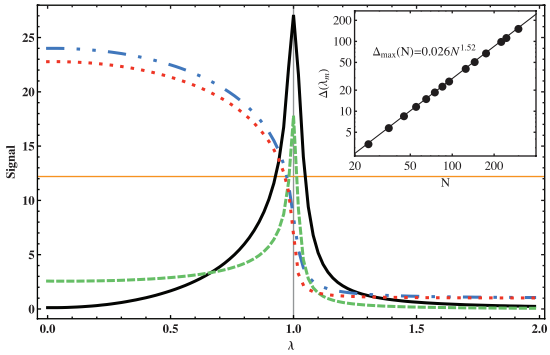

Fig. 4: (Color online) $n(0)$ and $\Delta(0,0)$ as a function of λ for $N = 95$ spins and two different anisotropies: The dot-dashed blue (red dotted) curves and solid black (dashed green) correspond to $n(0)$ and $\Delta(0,0)$ for $\gamma = 1 (\gamma = 0.5)$. The horizontal line at 12 is the maximal value that $\Delta(0,0)$ can take for a separable state and the peaks of $\Delta(0,0)$ exceed this threshold. The inset shows the numerical scaling of the $\Delta(0,0)$ peak *vs.* N which is in agreement with the analytic prediction of a power law with exponent 3/2.

$S_4(L) \leqslant 4$. While there is only a tiny enhancement of the entanglement entropy around the phase transition for $L = 1$, a peak grows with increasing separation L of the spins, and takes its maximum for $L \simeq N/4$, *i.e.* in the case of maximum separation. This behavior again gives evidence of the long-range character of the correlations.

Having defined proper entanglement quantifiers that capture the properties of a quantum phase transition, we now address the issue of how the latter can be linked to experimentally accessible observables. We focus our discussion on cold atomic systems, in view of their appeal as ideal quantum simulators of iconic condensed-matter Hamiltonians. In these systems absorption images taken after releasing the atoms from the trap are the most commonly used diagnostic tools. The average density profile after time of flight maps to the quasi-momentum distribution $n(q)$ of the atoms at the release time, and the density-density correlations (known as *noise correlations*) [30] yield the momentum-momentum correlation $\Delta(q_1, q_2)$. These functions are just Fourier transforms of two- and four-point correlations of the atomic-field creation and annihilation operators at the various lattice sites, $\hat{a}_n, \hat{a}_n^\dagger$:

$$n(q) \equiv \langle \hat{n}_q \rangle = \frac{1}{N} \sum_{n,m} e^{i\frac{2\pi}{N} q(n-m)} \langle \hat{a}_n^\dagger \hat{a}_m \rangle, \tag{3}$$

$$\Delta(q_1, q_2) \equiv \langle (\hat{n}_{q_1} - \langle \hat{n}_{q_1} \rangle)(\hat{n}_{q_2} - \langle \hat{n}_{q_2} \rangle) \rangle). \tag{4}$$

The noise correlations $\Delta(q_1, q_2)$ contain same non-local correlations as the ones included in T_4 and $S_4(L)$. However unlike T_4 and S_4, $\Delta(q_1, q_2)$ is not a proper entanglement monotone. On the other hand, unlike T_4 and S_4, $\Delta(q_1, q_2)$ can be measured experimentally. Therefore, the natural question that we address below is: how much information about the enhancement of many-body entanglement at the critical point can be inferred from noise correlations.

In view of the well-known mapping between hard-core bosons and spin-(1/2) operators [22], noise correlations for the spin chains can be defined by using the following relations between the spins and atomic operators: $\sigma_j^+ = \hat{a}_j^\dagger$, $\sigma_j^- = \hat{a}_j$ and $\sigma_j^z = 2\hat{a}_j^\dagger \hat{a}_j - 1$. In the following we use this mapping to study the behavior of $\Delta(0,0)$ and $n(0)$ as λ is varied across the critical point. Our aim is to use this exactly solvable system as a benchmark for the behavior of such correlations, which can be accessed experimentally in computationally intractable systems. Whereas their quantitative properties will depend on details of the underlying Hamiltonian, we believe that their qualitative features will be generic, due to the inherent universal scaling of a quantum phase transition.

Figure 4 shows that $\Delta(0,0)$ captures the enhancement of entanglement at the quantum critical point, whereas $n(0)$ does not. While $n(0)$ exhibits a step-like functional dependence of λ (similar to T_2), the noise autocorrelation function $\Delta(0,0)$ is sharply peaked near the critical point (similar to T_4). $\Delta(0,0)$ contains the higher-order non-local correlations which are the key to properly extract the enhancement of entanglement at the quantum phase transition.

Given the mapping between atomic and spin operators, separability of the atomic many-body states can also be probed via spin squeezing [31–36]. A separable state $|\Phi_s\rangle$ of a spin-(1/2) system is one that can be expressed in terms of one-body states $|\phi_i\rangle$ through $|\Phi_s\rangle = |\phi_1\rangle \otimes |\phi_2\rangle \otimes \ldots \otimes |\phi_N\rangle)$. As shown in the appendix the noise correlation $\Delta(0,0)$ satisfies

$$\Delta(0,0) < \Delta_{\max}(\Phi_s) = \frac{1}{8}(1+N). \tag{5}$$

Thus, if $\Delta(0,0)$ exceeds this threshold, the underlying state is entangled. In fig. 4 we display $\Delta_{\max}(\rho_s)$ for $N = 95$. The peak of $\Delta(0,0)$ clearly exceeds the separability threshold, by a factor that grows with the size of the system, N. The reason for this is as follows. While $\Delta(0,0)$ grows

algebraically as $N^{3/2}$, the separability threshold of eq. (5) is only linear in N, so that the excess of the peak over this threshold increases as $\sqrt{N}$. The exponent 3/2 in the noise correlation peak height follows from the universal scaling of $\langle\sigma_x\rangle \sim (\lambda-1)^{1/8}$, which yields a divergence of the noise correlation peak as $(\lambda-1)^{-3/2}$ in the thermodynamic limit and to a $N^{3/2}$ scaling for finite samples.

Even though the above investigations were focused on the anisotropic XY model Hamiltonian, we emphasize that eq. (5) provides a general criterion for arbitrary spin-(1/2) Hamiltonians and consequently corresponds to a useful benchmark to study entanglement properties in more general systems such as disordered spin chains or spins at finite temperature. Additionally, preliminary calculations done in in comparatively small 1D soft core bosons undergoing a superfluid–to–Mott-insulator transition [21,37] also indicate a similar peaked behavior of Δ close to the critical point. This suggests that the growth of Δ can be a generic signature of a quantum phase transition, and that noise correlations are suitable observables for experimental verification of the enhancement of entanglement.

* * *

FM and AMR respectively, acknowledge financial support by Alexander von Humboldt foundation and the ITAMP visitors program, and by the National Science Foundation.

Appendix

Given a separable state $|\Phi_s\rangle = |\phi_1\rangle \otimes |\phi_2\rangle \otimes \ldots \otimes |\phi_N\rangle$ of N spins $\Delta(0,0)$ can be decomposed into contributions of 1, 2 and 3 different atoms or spins: $\Delta(0,0) = \sum_{i_1} f^{(1)}_{i_1} + \sum_{i_1 i_2} f^{(2)}_{i_1 i_2} + \sum_{i_1 i_2} f^{(3)}_{i_1 i_2} + \sum_{i_1 i_2 i_3} f^{(4)}_{i_1 i_2 i_3}$, where the indices i_j label the spins, and all summations are performed over pairwise different indices. All contributions from four different spins vanish. More explicitly, $f^{(1)}$ to $f^{(4)}$ read

$$f^{(1)}_{i_1} = \langle a^\dagger_{i_1} a_{i_1} a^\dagger_{i_1} a_{i_1}\rangle - \langle a^\dagger_{i_1} a_{i_1}\rangle\langle a^\dagger_{i_1} a_{i_1}\rangle = \frac{1-z^2_{i_1}}{4} \leqslant \frac{1}{4}, \tag{A.1}$$

where the above mapping between atomic and spin operators has been performed. z_{i_1} is a short-hand notation for $\langle\phi_{i_1}|\sigma_z|\phi_{i_1}\rangle$, and x_{i_j} and y_{i_j} that will be used in the following are defined analogously.

$$f^{(2)}_{i_1 i_2} = \sum_{[ijkl]=\Pi[i_1 i_1 i_1 i_2]} \langle a^\dagger_i a_j a^\dagger_k a_l\rangle - \langle a^\dagger_i a_j\rangle\langle a^\dagger_k a_l\rangle \tag{A.2}$$

$$= \frac{1-z_{i_1}}{4}(x_{i_1}x_{i_2} + y_{i_1}y_{i_2}) \tag{A.3}$$

$$\leqslant \frac{1-z_{i_1}}{4}\sqrt{x^2_{i_1}+y^2_{i_1}}\sqrt{x^2_{i_2}+y^2_{i_2}} \tag{A.4}$$

$$= \frac{1-z_{i_1}}{4}\sqrt{1-z^2_{i_1}}\sqrt{1-z^2_{i_2}} \tag{A.5}$$

$$\leqslant \frac{1-z_{i_1}}{8}((1-z^2_{i_1})+(1-z^2_{i_2})). \tag{A.6}$$

Here, $\Pi[i_1 i_1 i_1 i_2]$ denotes all permutations of, *i.e.* $[i_1,i_1,i_1,i_2]$, $[i_1,i_1,i_2,i_1]$, $[i_1,i_2,i_1,i_1]$, $[i_2,i_1,i_1,i_1]$. The Cauchy-Schwartz inequality leads from eq. (A.3) to eq. (A.4); eq. (A.5) follows since $x^2_{i_j}+y^2_{i_j}+z^2_{i_j}$ equals unity for a pure state $|\phi_{i_j}\rangle$, and eq. (A.6) follows from $2ab \leqslant a^2+b^2$.

$$f^{(3)}_{i_1 i_2} = \sum_{[ijkl]=\Pi[i_1 i_1 i_2 i_2]} \langle a^\dagger_i a_j a^\dagger_k a_l\rangle - \langle a^\dagger_i a_j\rangle\langle a^\dagger_k a_l\rangle \tag{A.7}$$

$$= \frac{1}{16}(4-(x^2_{i_1}+y^2_{i_1})(x^2_{i_2}+y^2_{i_2}) - 4z_{i_1}z_{i_2}) \tag{A.8}$$

$$= \frac{1}{16}(4-(1-z^2_{i_1})(1-z^2_{i_2}) - 4z_{i_1}z_{i_2}). \tag{A.9}$$

$$f^{(4)}_{i_1 i_2 i_3} = \sum_{[ijkl]=\Pi[i_1 i_1 i_2 i_3]} \langle a^\dagger_i a_j a^\dagger_k a_l\rangle - \langle a^\dagger_i a_j\rangle\langle a^\dagger_k a_l\rangle \tag{A.10}$$

$$= \frac{1}{8}(2-x^2_{i_1}-y^2_{i_1})(x_{i_2}x_{i_3}+y_{i_2}y_{i_3}) \tag{A.11}$$

$$\leqslant \frac{1}{8}(1+z^2_{i_1})\sqrt{x^2_{i_2}+y^2_{i_2}}\sqrt{x^2_{i_3}+y^2_{i_3}} \tag{A.12}$$

$$= \frac{1}{8}(1+z^2_{i_1})\sqrt{1-z^2_{i_2}}\sqrt{1-z^2_{i_3}} \tag{A.13}$$

$$\leqslant \frac{1}{16}(1+z^2_{i_1})((1-z^2_{i_2})+(1-z^2_{i_3})). \tag{A.14}$$

Here, similar estimates as from eq. (A.3) to eq. (A.6) have been done. Since $\Delta(0,0)$ is obtained via a sum of the $f^{(j)}$ over all indices, one can replace these expressions by their symmetrized versions:

$$\left[f^{(2)}_{i_1 i_2}\right]_s \leqslant \frac{2-z_{i_1}-z_{i_2}}{16}((1-z^2_{i_1})+(1-z^2_{i_2})), \tag{A.15}$$

$$\left[f^{(4)}_{i_1 i_2 i_3}\right]_s \leqslant \frac{1}{24}(3-z^2_{i_1}z^2_{i_2}-z^2_{i_2}z^2_{i_3}-z^2_{i_2}z^2_{i_3}). \tag{A.16}$$

The maximum of $[f^{(2)}_{i_1 i_2}]_s + f^{(3)}_{i_1 i_2}$ is obtained for $z_{i_1}=1$, $z_{i_2}=-1$, and it amounts to 1/2. The maximum of $[f^{(4)}_{i_1 i_2 i_3}]_s$ is obtained for $z_{i_1}=z_{i_2}=z_{i_3}=0$, and it amounts to 1/8. Summing up these estimates yields eq. (5).

REFERENCES

[1] Nielsen M. and Chuang I., *Quantum Computation and Quantum Communication* (Cambridge University Press, Cambridge) 2000.
[2] Wu L.-A., Sarandy M. S. and Lidar D. A., *Phys. Rev. Lett.*, **93** (2004) 250404.
[3] Roscilde T. *et al.*, *Phys. Rev. Lett.*, **94** (2005) 147208.
[4] Venuti L. C. *et al.*, *Phys. Rev. B*, **78** (2008) 115410.
[5] Vollbrecht K. G. H. and Cirac J. I., *Phys. Rev. Lett.*, **98** (2007) 190502.
[6] Amico L. *et al.*, *Rev. Mod. Phys.*, **80** (2008) 517.
[7] Osterloh A. *et al.*, *Nature*, **416** (2002) 608.
[8] Osborne T. J. and Nielsen M. A., *Phys. Rev. A*, **66** (2002) 032110.
[9] Latorre J. I. *et al.*, *Quantum Inf. Comput.*, **4** (2004) 48.
[10] Vidal G. *et al.*, *Phys. Rev. Lett.*, **90** (2003) 227902.

[11] de Oliveira T. R. *et al.*, *Phys. Rev. Lett.*, **97** (2006) 170401.
[12] de Oliveira T. R., Rigolin G. and de Oliveira M. C., *Phys. Rev. A*, **73** (2006) 010305(R).
[13] de Oliveira T. R. *et al.*, *Phys. Rev. A*, **77** (2008) 032325.
[14] Greiner M. *et al.*, *Nature*, **415** (2002) 39.
[15] Foelling S. *et al.*, *Nature*, **434** (2005) 481.
[16] Spielman I. B. *et al.*, *Phys. Rev. Lett.*, **98** (2007) 080404.
[17] Sachdev S., *Quantum Phase Transitions* (Cambridge University Press, Cambridge) 1999.
[18] Johnson J. D. and McCoy B. M., *Phys. Rev. A*, **4** (1971) 2314.
[19] Lieb E. H. and Liniger W., *Phys. Rev.*, **130** (1963) 1605.
[20] Lieb E., Schultz T. and Mattis D., *Ann. Phys. (N.Y.)*, **16** (1961) 407.
[21] Rey A. M., Satija I. I. and Clark C. W., *J. Phys. B: At. Mol. Opt. Phys.*, **39** (2006) S177.
[22] Holstein T. and Primakoff H., *Phys. Rev.*, **58** (1940) 1098.
[23] Hill S. and Wootters W. K., *Phys. Rev. Lett.*, **78** (1997) 5022.
[24] Wootters W. K., *Phys. Rev. Lett.*, **80** (1998) 2245.
[25] Rungta P. *et al.*, *Phys. Rev. A*, **64** (2001) 042315.
[26] Mintert F., Kuś M. and Buchleitner A., *Phys. Rev. Lett.*, **95** (2005) 260502.
[27] Meyer D. A. and Wallach N. R., *J. Math. Phys*, **43** (2002) 4273.
[28] Scott A. J., *Phys. Rev. A*, **69** (2004) 052330.
[29] Carvalho A. R. R., Mintert F. and Buchleitner A., *Phys. Rev. Lett.*, **93** (2004) 230501.
[30] Altman E. *et al.*, *Phys. Rev. A*, **70** (2004) 013603.
[31] Sørensen A., Duan L.-M., Cirac J. I. and Zoller P., *Nature*, **409** (2001) 63.
[32] Gühne O. and Lewenstein M., *Phys. Rev. A*, **70** (2004) 022316.
[33] Korbicz J. K., Cirac J. I. and Lewenstein M., *Phys. Rev. Lett.*, **95** (2005) 120502.
[34] Korbicz J. K., Gühne O., Lewenstein M., Häffner H., Roos C. F. and Blatt R., *Phys. Rev. A*, **74** (2006) 052319.
[35] Tóth G. and Gühne Otfried, *Appl. Phys. B*, **82** (2006) 237.
[36] Tóth G., Christian Knapp, Otfried Gühne and Briegel Hans J., *Phys. Rev. Lett*, **99** (2007) 250405.
[37] Rey A. M., Satija I. I. and Clark C. W., *New J. Phys.*, **8** (2006) 155.